Electronic Supplementary Information (ESI) for Nanoscale
This journal is © The Royal Society of Chemistry 2023

Plasmon photocatalytic CO_2 reduction reactions over Au particles on various substrates

Kai Wang[a,b] and Tao He*[a,b]

[a] *CAS Key Laboratory of Nanosystem and Hierarchical Fabrication, National Center for Nanoscience and Technology, Beijing 100190, China. E-mail: het@nanoctr.cn*

[b] *University of Chinese Academy of Sciences, Beijing 100049, China.*

Fig. S1. Size distribution of Au particles on the substrates of (a) Au-SiO_2, (b) Au-n-Si, (c) Au-p-Si, (d) Au-TiO_2-SiO_2, (e) Au-TiO_2-n-Si, and (f) Au-TiO_2-p-Si.

Fig. S2. Histograms of size statistics for Au particles on the substrates of (a-f) Au-SiO_2, (b) Au-n-Si, (c) Au-p-Si, (d) Au-TiO_2-SiO_2, (e) Au-TiO_2-n-Si, and (f) Au-TiO_2-p-Si, indicating the size of majority particles is (20±5) nm for all the samples.

Fig. S3. Optical refractive index and extinction coefficient for different substrates of (a-c) SiO_2, (b) n-Si, and (c) p-Si. The inset diagrams of (b-c) show the bandgap of n-Si and p-Si, respectively.

Fig. S4. Optical properties of TiO_2 on the substrates of SiO_2, n-Si and p-Si. (a) Refractive index and extinction coefficient spectra, (b) real and imaginary parts of dielectric constant, and (c-e) bandgap determination of TiO_2 from extinction coefficient spectra.

Fig. S5. Optical properties of Au on the substrates of SiO_2, n-Si and p-Si. Spectra of (a) refractive index, (b) extinction coefficient, and (c) real and (d) imaginary parts of dielectric constant.

Fig. S6. Optical properties of Au/TiO_2 on the substrates of SiO_2, n-Si and p-Si. Spectra of (a) refractive index, (b) extinction coefficient, (c) real and (d) imaginary parts of dielectric constant.

Fig. S7. UV-vis absorption spectrum of 10^{-6} mol/L R6G with a strong absorption peak at 527 nm.

Fig. S8. Photoelectrochemical characteristics of Au and Au/TiO_2 on n-Si. (a) Transient photocurrent density vs time for different samples and (b) schematic diagram of photocurrent generation and charge transfer for Au-TiO_2-n-Si sample under visible-light illumination.

Fig. S9. Temperature distribution on the sample surface of (a,b) SiO_2 and (c,d) Au-SiO_2 (a,c) before and (b,d) after visible-light irradiation.

Fig. S10. Alignment of energy levels for R6G, Au, Si, TiO_2 and SiO_2, with respect to the level of vacuum (left) and NHE (right). The red dashed lines are the respective redox potentials of CO_2/CO and CO_2/CH_4.

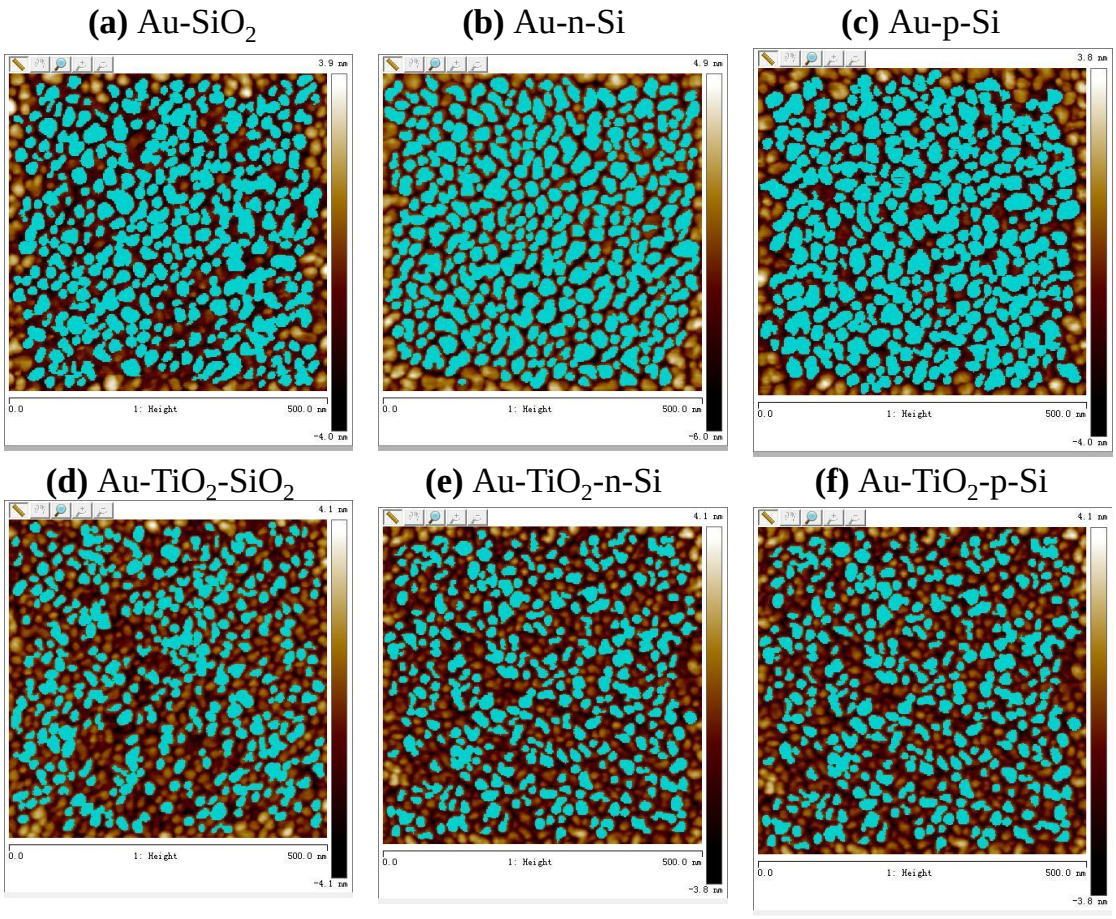

Fig. S1. Size distribution of Au particles on the substrates of (a) Au-SiO_2, (b) Au-n-Si, (c) Au-p-Si, (d) Au-TiO_2-SiO_2, (e) Au-TiO_2-n-Si, and (f) Au-TiO_2-p-Si.

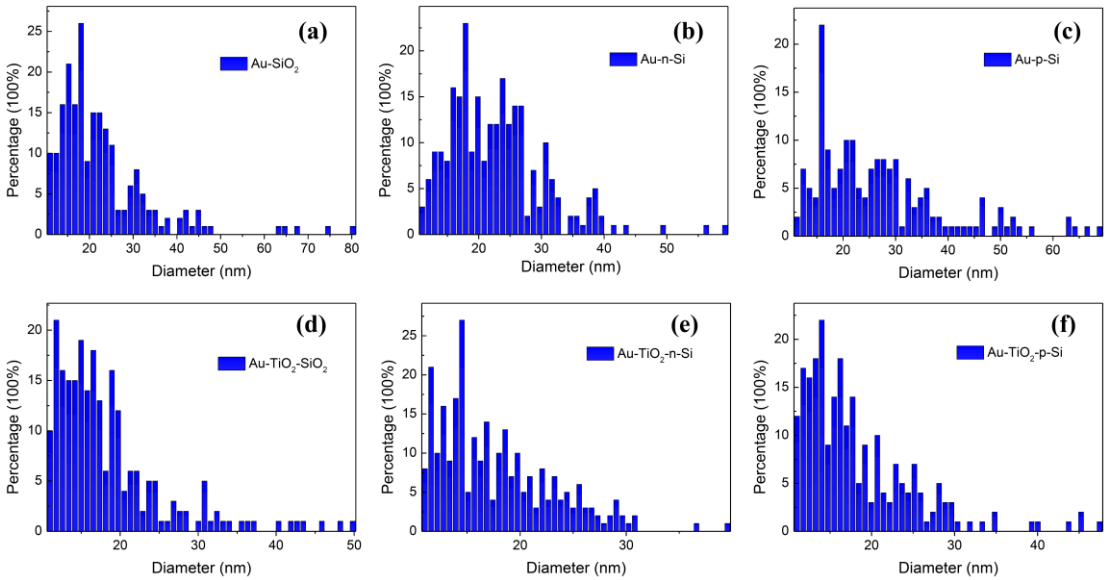

Fig. S2. Histograms of size statistics for Au particles on the substrates of (a-f) Au-SiO_2, (b) Au-n-Si, (c) Au-p-Si, (d) Au-TiO_2-SiO_2, (e) Au-TiO_2-n-Si, and (f) Au-TiO_2-p-Si, indicating the size of majority particles is (20$\pm$5) nm for all the samples.

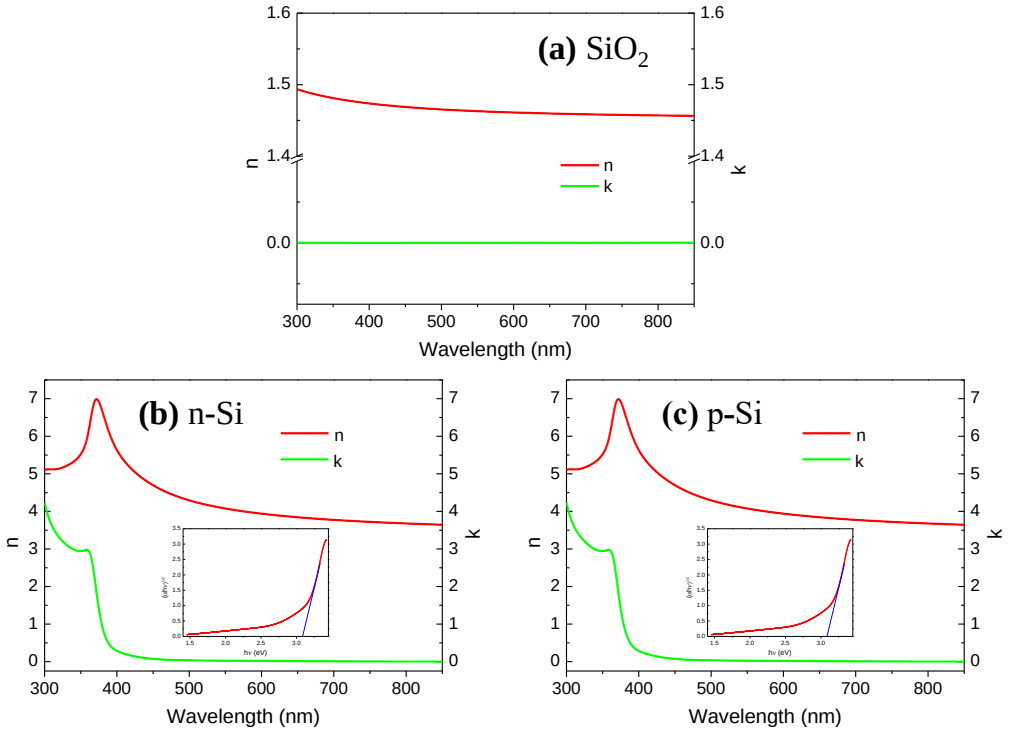

Fig. S3. Optical refractive index and extinction coefficient for different substrates of (a-c) SiO_2, (b) n-Si, and (c) p-Si. The inset diagrams of (b-c) show the bandgap of n-Si and p-Si, respectively.

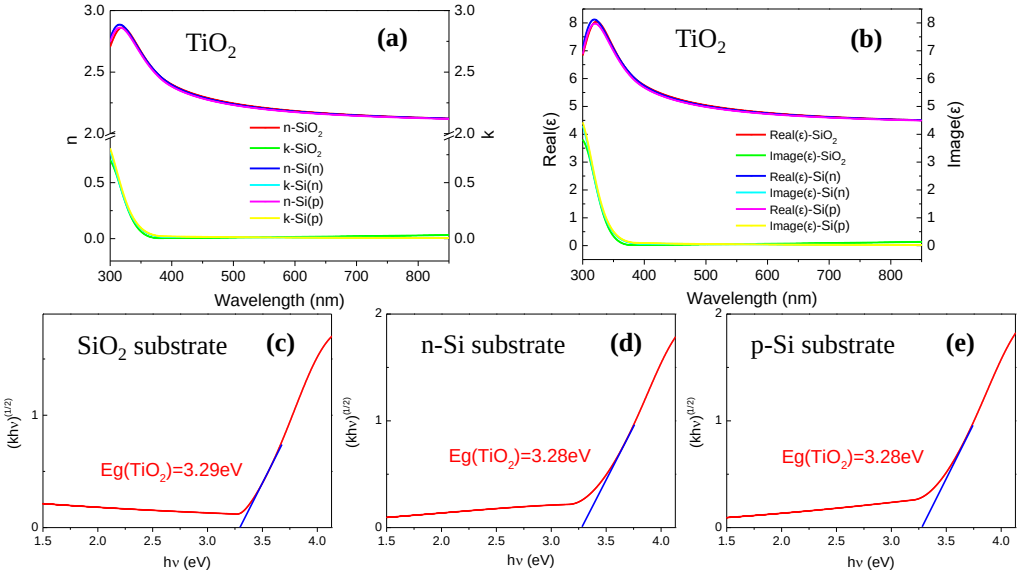

Fig. S4. Optical properties of TiO_2 on the substrates of SiO_2, n-Si and p-Si. (a) Refractive index and extinction coefficient spectra, (b) real and imaginary parts of dielectric constant, and (c-e) bandgap determination of TiO_2 from extinction coefficient spectra.

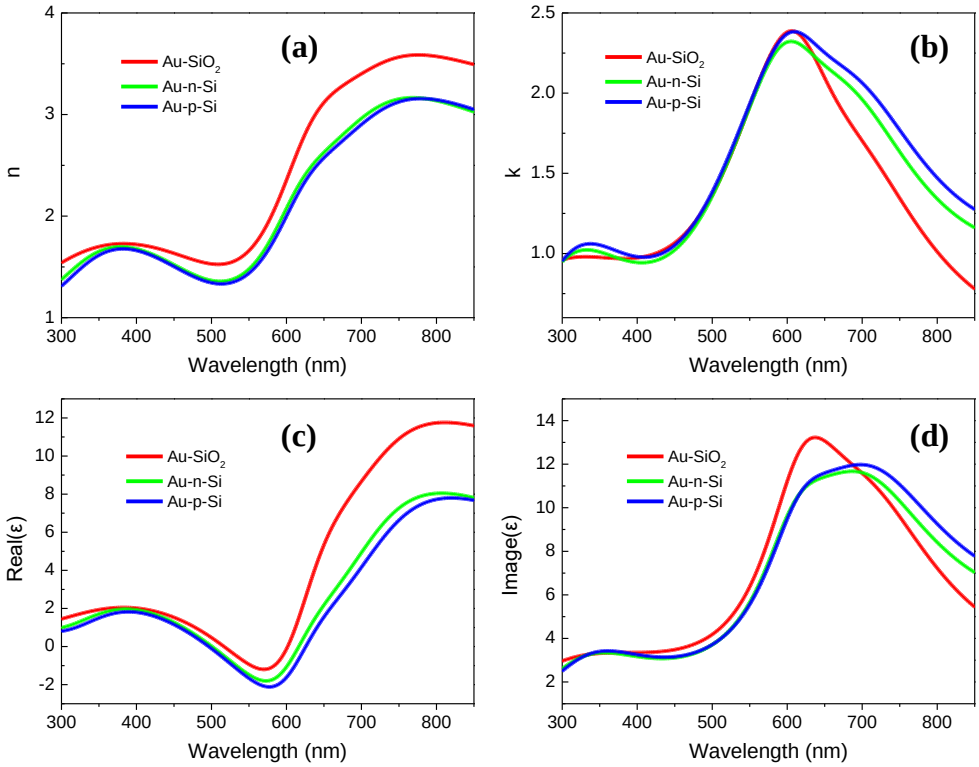

Fig. S5. Optical properties of Au on the substrates of SiO_2, n-Si and p-Si. Spectra of (a) refractive index, (b) extinction coefficient, and (c) real and (d) imaginary parts of dielectric constant.

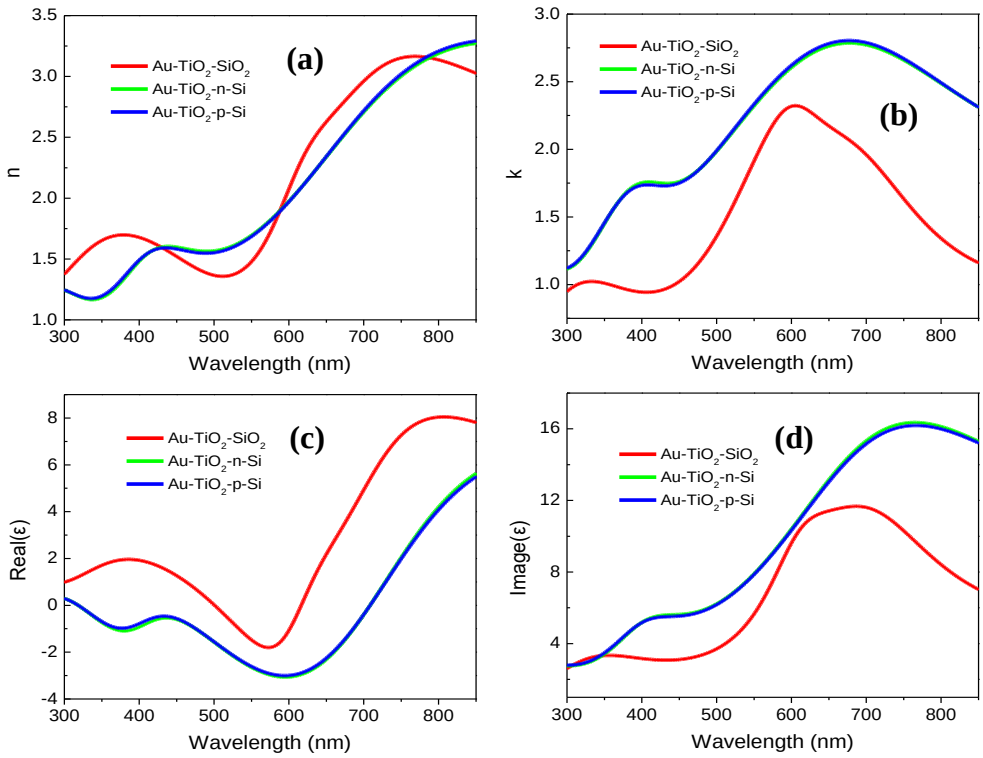

Fig. S6. Optical properties of Au/TiO_2 on the substrates of SiO_2, n-Si and p-Si. Spectra of (a) refractive index, (b) extinction coefficient, (c) real and (d) imaginary parts of dielectric constant.

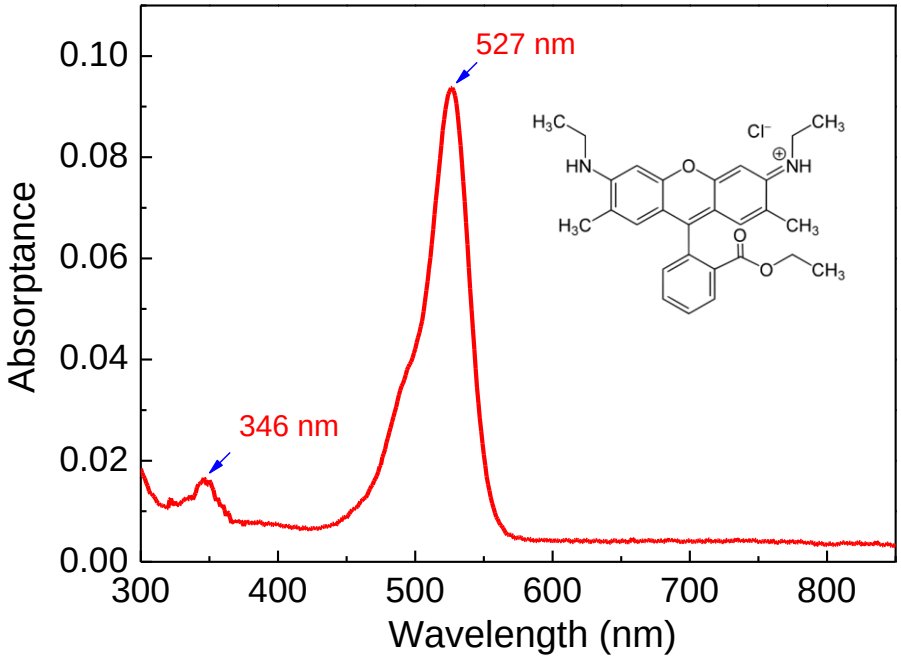

Fig. S7. UV-vis absorption spectrum of 10^{-6} mol/L R6G with a strong absorption peak at 527 nm.

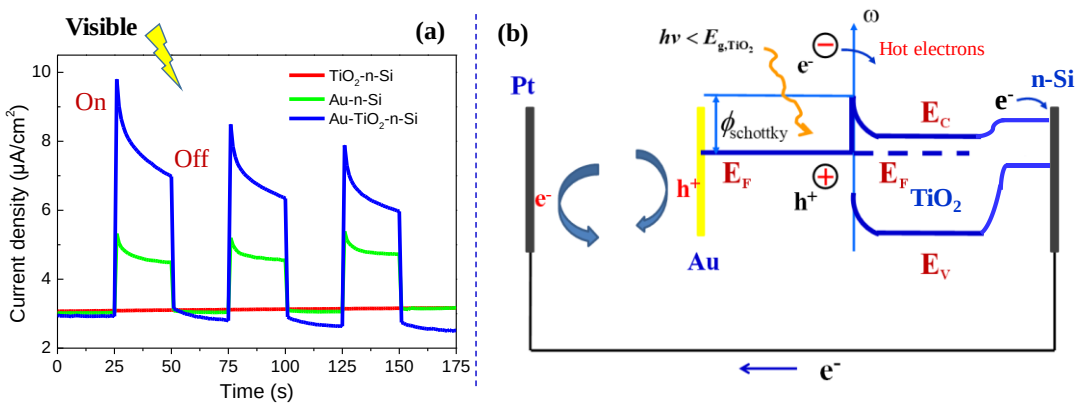

Fig. S8. Photoelectrochemical characteristics of Au and Au/TiO_2 on n-Si. (a) Transient photocurrent density vs time for different samples and (b) schematic diagram of photocurrent generation and charge transfer for Au-TiO_2-n-Si sample under visible-light illumination.

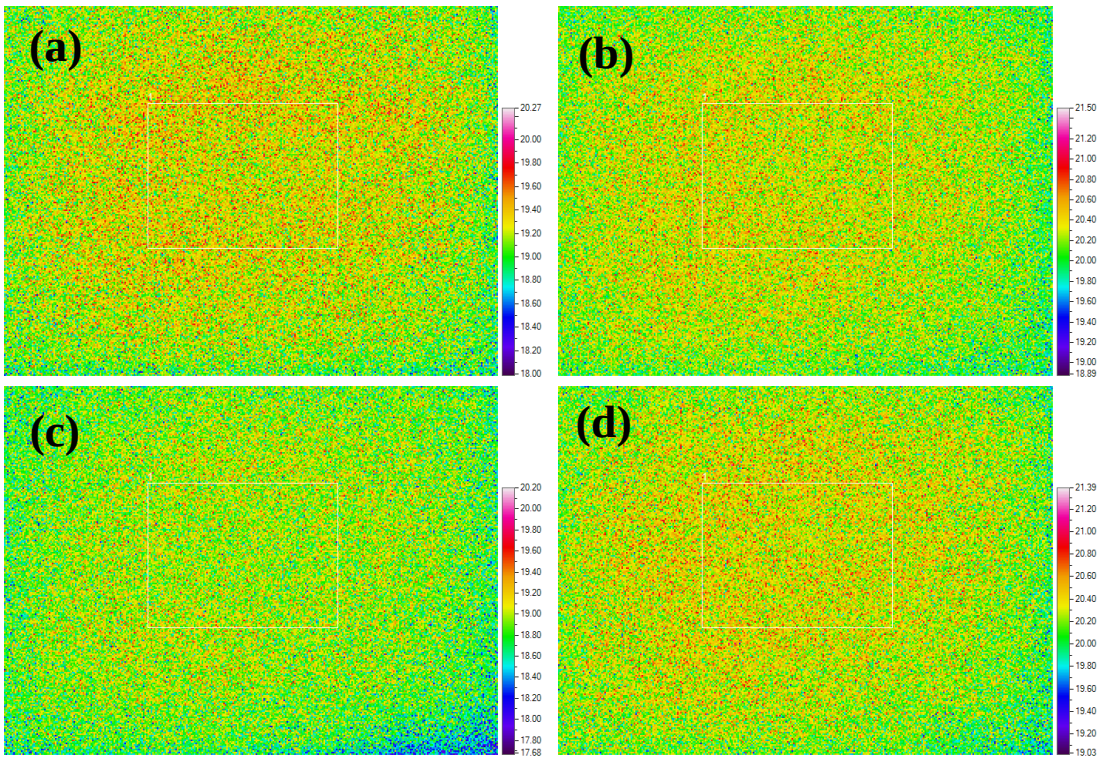

Fig. S9. Temperature distribution on the sample surface of (a,b) SiO_2 and (c,d) Au-SiO_2 (a,c) before and (b,d) after visible-light irradiation.

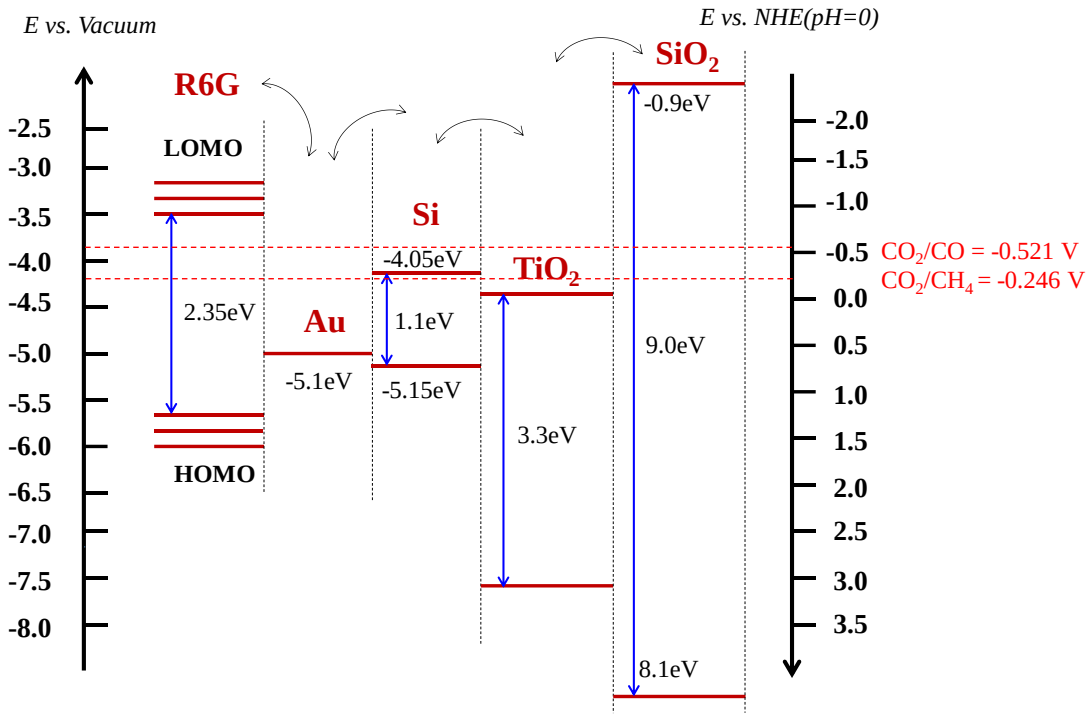

Fig. S10. Alignment of energy levels for R6G, Au, Si, TiO_2 and SiO_2, with respect to the level of vacuum (left) and NHE (right). The red dashed lines are the respective redox potentials of CO_2/CO and CO_2/CH_4.